ChemPhysChem

Research Article
doi.org/10.1002/cphc.202400011

Chemistry Europe
European Chemical Societies Publishing

www.chemphyschem.org

Hydrogen Bonding and Molecular Geometry in Isolated Hydrates of 2-Ethylthiazole Characterised by Microwave Spectroscopy

Charlotte N. Cummings[a] and Nicholas R. Walker*[a]

Broadband microwave spectra of the isolated 2-ethylthiazole molecule, and complexes of 2-ethylthiazole···H_2O and 2-ethylthiazole···$(H_2O)_2$ have been recorded by probing a gaseous sample containing low concentrations of 2-ethylthiazole and water within a carrier gas undergoing supersonic expansion. The identified conformer of the isolated 2-ethylthiazole molecule and the 2-ethylthiazole sub-unit within each of 2-ethylthiazole···H_2O and 2-ethylthiazole···$(H_2O)_2$ have C_1 symmetry. The angle that defines rotation of the ethyl group relative to the plane of the thiazole ring, ∠(S-C2-C6-C7), is −98.6(10)° within the isolated 2-ethylthiazole molecule. Analysis of molecular geometries and non-covalent interactions reveals each hydrate complex contains a non-linear primary, N···H_b-O, hydrogen bond between an O–H of H_2O and the nitrogen atom while the O atom of the water molecule(s) interacts weakly with the ethyl group. The ∠(H_b···N-C2) parameter, which defines the position of the H_2O molecule relative to the thiazole ring, is found to be significantly greater for 2-ethylthiazole···H_2O than for thiazole···H_2O. The distance between the O atoms is determined to be 2.894(21) Å within the dihydrate complex which is shorter than observed within the isolated water dimer. The primary hydrogen bond within 2-ethylthiazole···$(H_2O)_2$ is shorter and stronger than that in 2-ethylthiazole···H_2O as a result of cooperative hydrogen bonding effects.

Introduction

Nitrogen-containing heteroaromatic rings are important building blocks of biomolecules which have multiple binding sites for intermolecular interactions. Thiazole is present in many naturally occurring and synthetic compounds such as Vitamin B1 and epothilones (potential anti-cancer drugs). Imidazole is present within the DNA and RNA nucleobases, adenine and guanine, as well as in the amino acid, histamine. The study of complexes formed between thiazole, imidazole and their derivatives with small molecules such as water provide an insight into the binding preferences of these molecules. Microwave spectroscopy is a powerful technique able to distinguish fine details of molecular structure for molecules and complexes isolated in the gas phase, free of solvent or matrix effects. Each of imidazole and thiazole has a pyridinic nitrogen which can accept hydrogen bonds. Recent microwave spectroscopic studies of B···H_2O complexes (where B is either imidazole,[1] methylimidazole,[2] thiazole[3] or methylthiazole)[4] have revealed that the lowest-energy isomer of a 1:1 complex formed between B and H_2O typically features a pair of hydrogen bonding interactions. A comparatively strong hydrogen bond forms between O–H of H_2O and the pyridinic nitrogen on the heteroaromatic ring while a weaker hydrogen bond forms between the O of H_2O and a hydrogen atom or CH_3 group attached to the 2- or 4-position of the ring. The present work reports and analyses microwave spectra of the 2-ethylthiazole molecule and of isolated complexes of 2-ethylthiazole···H_2O and 2-ethylthiazole···$(H_2O)_2$ (hereafter referred to as 2-ET, 2-ET···H_2O and 2-ET···$(H_2O)_2$ respectively). It explores how the configuration of hydrogen bonds within the complexes is influenced by the alkyl group at the 2-position of the ring. It examines how the attachment of H_2O to 2-ethylthiazole affects the conformational preferences of the ethyl group. The calculated geometries of the lowest-energy conformers of each of the species studied by this work are presented in Figure 1.

The lowest-energy conformers of ethylated derivatives of each of benzene,[5] aniline[6] and furan[7] have been observed by microwave spectroscopy. Conformers of these molecules of C_s symmetry have both carbon atoms of the ethyl group co-planar with the aromatic ring. Conformers that have C_1 symmetry have one or more carbon atoms lying outside of the ring plane. The dihedral angle that defines rotation about the C–C bond which connects the ethyl group with the aromatic ring (analogous to ∠(C7-C6-C2-N) in the C_1 conformation of 2-ethylthiazole shown in Figure 1) was found to be close to 90° for the lowest-energy (C_1) conformers of each of ethylbenzene, 3-ethylaniline and 4-ethylaniline. It was found to be 75.6(8)° and 63.31(64)° for the observed C_1 conformers of each of 2-ethylaniline and 2-ethylfuran respectively (in the r_s geometries). Both C_s and C_1 conformers (one conformer of each symmetry) were observed during microwave spectroscopy experiments which probed 2-ethylfuran entrained within helium undergoing supersonic expansion. The difference between the results of ~90° for 3-

[a] C. N. Cummings, N. R. Walker
Chemistry- School of Natural and Environmental Sciences, Newcastle University, Bedson Building NE1 7RU, U.K
E-mail: nick.walker@newcastle.ac.uk

Supporting information for this article is available on the WWW under https://doi.org/10.1002/cphc.202400011

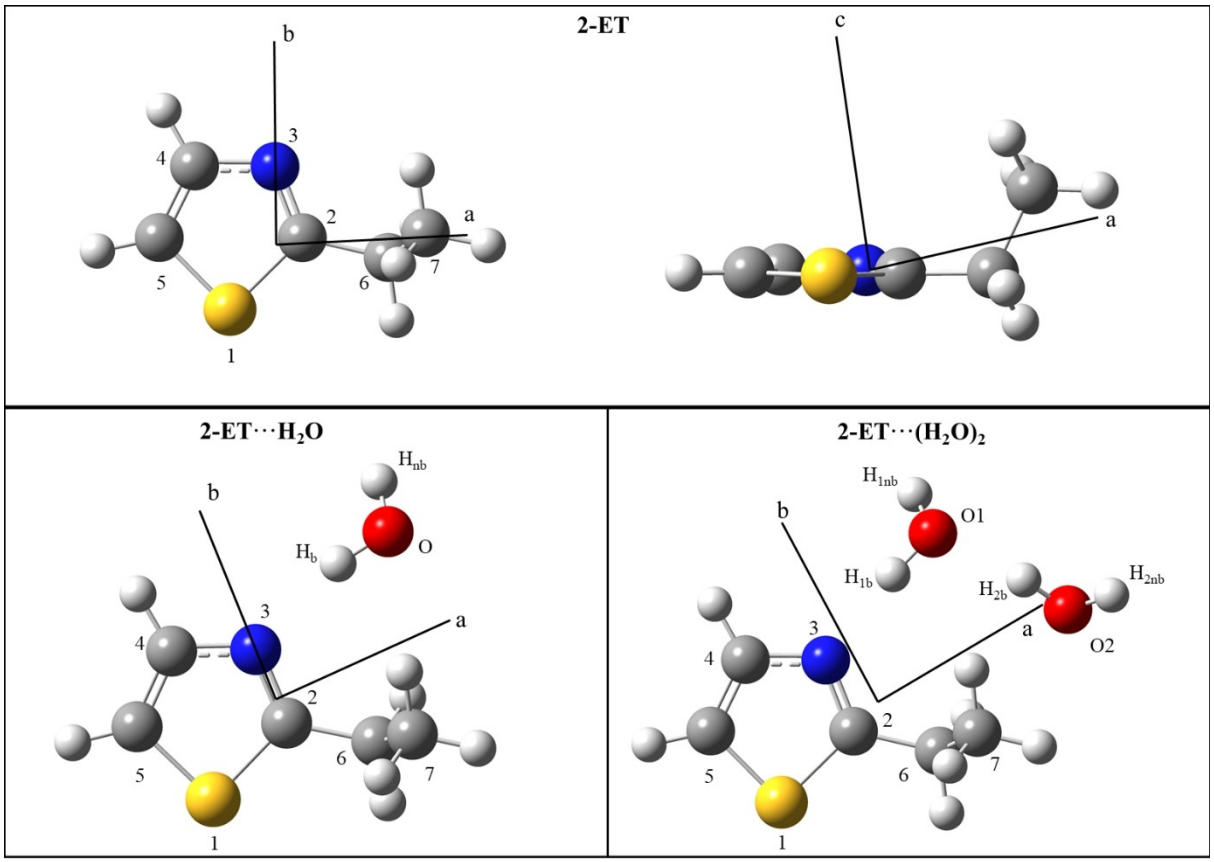

Figure 1. Equilibrium (r_e) geometries of 2-ET (upper panel), 2-ET···H_2O and 2-ET···$(H_2O)_2$ (lower panel) calculated at the ωB97X-D/aug-cc-pVQZ level of theory.

ethylaniline/4-ethylaniline and that of 75.6(8)° for 2-ethylaniline was rationalised by invoking the presence of a weak hydrogen bond between the nitrogen atom of the aniline group and the ethyl chain. It will be shown that ∠(C7-C6-C2-N) for 2-ethylthiazole also deviates from 90° in similarity with the results obtained for 2-ethylaniline and 2-ethylfuran.

The binding of H_2O to each of imidazole[1] and thiazole[3] has been studied within a series of recent works. Interest has recently focussed on effects of the weak hydrogen bond formed between the H_2O sub-unit and the neighbouring atom or group located on the 2- or 4- position of the ring. It was shown that the (V_3) barriers to internal rotation of the CH_3 group within each of *N*-methylimidazole···H_2O[2], 4-methylthiazole···H_2O[4] and 5-methylthiazole···H_2O[4] are very similar to those within the respective *N*-methylimidazole,[8] 4-methylthiazole[9] and 5-methylthiazole[10] monomers. There is a significant *increase* in V_3 on the attachment of H_2O to 2-methylimidazole which was attributed to the effect of a weak hydrogen bond between the O of H_2O and the CH_3 group attached to the 2-position of the ring.[2] There is a *decrease* in V_3 on the attachment of H_2O to 4-methylthiazole which may arise because minor changes in electronic structure within the ring accompany formation of the monohydrate from the isolated sub-units. In context of the described studies of monohydrates of methylated heteroaromatics, the significance of the present work is that it extends the range of systems characterised to include the mono- and dihydrate of a heteroaromatic that contains an alkyl group in the 2-position which is able to interact with the coordinating H_2O molecule. The geometries of binding interactions within each of 2-ET···H_2O and 2-ET···$(H_2O)_2$ will be shown to be similar to those in thiazole···H_2O, 2-methylimidazole···H_2O and thiazole···$(H_2O)_2$ (isomer I).[11] The broad picture is that H_2O molecules which hydrate imidazole and thiazole significantly affect the conformational and internal dynamics of substituents in the 2- and 4-positions of these heterocycles through weak hydrogen-bonding interactions.

Experimental and Theoretical Methods

Experiments and Instruments

A commercially-obtained sample of 2-ET (TCI Chemicals) was used for experiments without any further purification. 2-ET is liquid at ambient temperature and pressure, has vapour pressure of 6.0 mmHg at 25 °C and was initially vaporised from a reservoir[12] at 70 °C to seed a low concentration into the flow of an inert carrier gas. The carrier gas was either argon (BOC, 99.998 %) at a backing pressure of 3 bar or neon (BOC, CP grade) at 4 bar. A second reservoir positioned downstream of the first was used to introduce a low concentration of water into the carrier gas flow. The resulting gas mixture was introduced into a vacuum chamber by supersonic expansion from a pulsed gas injection nozzle (0.7 mm orifice) operated at approximately 2 Hz. Molecules were thus cooled to low rotational temperatures (~3 K) allowing weakly-bound complexes to

form within the expanding gas sample. Experiments to study D- and ^{18}O-containing isotopologues were facilitated by the introduction of either D_2O (Sigma Aldrich, 99.9% D atom) or $H_2{}^{18}O$ (Sigma Aldrich, 97% ^{18}O atom) into the gas flow from the second reservoir. Low concentrations of $H_2{}^{16}O$ were present as a contaminant during these experiments permitting the study of mixed isotopologues such as 2-ET···HDO and 2-ET···($H_2{}^{16}O$)($H_2{}^{18}O$).

Transitions in the rotational spectra of 2-ET, 2-ET···H_2O and 2-ET···$(H_2O)_2$ were measured concurrently owing to the broad bandwidth of the Chirped-Pulse Fourier Transform Microwave (CP-FTMW) spectrometer employed. The spectrometer was slightly re-configured between experiments that separately probed the 2–8 GHz and 7.0–18.5 GHz frequency ranges, a detailed description of the spectrometer is provided elsewhere.[13,14] Experiments performed in the lower frequency range used 2–8 GHz chirped pulses of 1 microsecond in duration generated by an Arbitrary Waveform Generator (Tektronix AWG7102). These were amplified by a 450 W Travelling Wave Tube (TWT) Amplifier (Applied Systems Engineering) prior to their introduction into the vacuum chamber from a horn antenna. The axes of the expanding gas jet and the introduced microwave radiation were oriented to be mutually perpendicular and intersecting. On resonance with an introduced microwave pulse, polar molecules and complexes within the gas jet became rotationally-polarised. Free induction decays (FID's) of 20 μs in duration were recorded at a second horn antenna. Eight FID's per nozzle pulse were digitally recorded by a 100 GS s^{-1} oscilloscope (Tektronix DPO72304XS) and co-added in the time domain before Fourier transformation of the data using either a Kaiser-Bessel or High Resolution window function.[15] Full details of the High Resolution window function are given in the supplementary information of reference 15.

Experiments performed in the upper frequency range used a chirped microwave pulse spanning from 0.5–12 GHz that was mixed against a 19 GHz reference signal provided by a Phase Locked Dielectric Resonant Oscillator (PDRO) to generate the 7.0–18.5 GHz chirped pulse. The lower frequency sideband (7.0–18.5 GHz) was selected by a low pass filter and the higher frequency sideband (19.5–31 GHz) was removed using a filter. A 300 W TWT amplifier (AR UK Ltd) was used to generate the amplified, chirped pulse. FID's of the molecular emission were detected by the 2nd horn antenna before mixing down against the 19 GHz reference prior to recording and co-addition of the FID's by the oscilloscope. Experiments in each frequency range achieved a linewidth of 100 kHz for an isolated line at full-width half maximum. Line centres in the frequency domain spectrum have an estimated accuracy of 10 kHz. Accuracy in transition frequencies and phase reproducibility during signal averaging were provided by a Rb-clock (SRS FS725) or an Analog Signal Generator (Agilent MXG N5183 A) to which the AWG, PDRO and oscilloscope were phase-locked.

Quantum Chemical Calculations

Quantum chemical calculations were performed using the Gaussian09 package.[16] Microwave spectroscopy experiments[7] to study 2-ethylfuran observed multiple low-energy conformers that are distinct by virtue of the degree of rotation of the ethyl group relative to the plane of the ring (as defined by the dihedral coordinate analogous to the ∠(C7-C6-C2-N) coordinate of 2-ET). One-dimensional relaxed potential energy scans (PES) were therefore performed while varying ∠(C7-C6-C2-N) for the isolated 2-ET molecule. Each scan measured the potential energy over a range of angles separated by 5° intervals. Scan calculations were performed using the harmonic hybrid function[17–19] of Becke, Lee, Yang and Parr (B3LYP), in conjunction with Grimme's dispersion correlation effects[20] and Becke-Jonhson damping function,[21,22] D3BJ, alongside either Dunning's augmented triple-ζ aug-cc-pVTZ basis set,[23,24] B3LYP(D3BJ)/aug-cc-pVTZ, or Ahlrichs'[25,26] valence polarized Def2-TZVP basis set, B3LYP(D3BJ)/Def2-TZVP. An additional scan calculation was also performed using second order Møller–Plesset perturbation theory[27] with Dunning's augmented double-ζ aug-cc-pVDZ basis set, MP2/aug-cc-pVDZ. As shown by Figure 2, each calculation predicted two degenerate minima which each have C_1 symmetry. At the B3LYP(D3BJ)/aug-cc-pVTZ level, the molecular geometries implied by these minima have ∠(C7-C6-C2-N) = ±85° such that they are interchanged by reflection through the horizontal symmetry plane of the thiazole ring. Very similar results were obtained using each of the theoretical methods employed. Optimisation of the global minimum structure of 2-ET was performed at each level of theory listed above and also by use of the long-range corrected hybrid functional,[28] ωB97X-D, with Dunning's quadrupole-ζ aug-cc-pVQZ basis set. The described exploration of the conformational landscape for the isolated 2-ET molecule provided a good foundation for the calculations subsequently performed on the 2-ET···H_2O and 2-ET···$(H_2O)_2$ complexes.

When calculating the optimised geometries of 2-ET···H_2O and 2-ET···$(H_2O)_2$, it was first assumed that the 2-ET sub-unit adopts a C_1 geometry within each complex. Other assumptions were informed by previous studies of thiazole-containing hydrate complexes. Calculations performed for each of 2-ET···H_2O and 2-ET···$(H_2O)_2$ initially placed one water molecule near to the nitrogen atom oriented so as to allow for a hydrogen bond between an O–H of H_2O and the N atom. The second H_2O of 2-ET···$(H_2O)_2$ was positioned and oriented to allow for an O···H–O hydrogen bond to form with the first H_2O. The molecular geometries of the mono- and dihydrate were optimised at the same levels of theory as were used for the isolated 2-ET molecule. Each complex was calculated to be a near-prolate asymmetric top with the strongest dipole moment component being along the *a*-inertial axis. The optimised geometries of 2-ET, 2-ET···H_2O and 2-ET···$(H_2O)_2$ calculated at the ωB97X-D/aug-cc-pVQZ level are shown in Figure 1. Calculated equilibrium rotational constants (A_e, B_e, C_e), nuclear quadrupole coupling constants (χ_{aa}(N), [χ_{bb}(N)–χ_{cc}(N)]) and electric dipole moment components ($|\mu_a|$, $|\mu_b|$, $|\mu_c|$) are summarised in Tables S1–S3 with atomic coordinates and illustrations of atom positions provided in Tables S4–S15.

Results

Spectral Analysis

Transitions of a C_1 conformer of the isolated 2-ET molecule (in a molecular geometry consistent with that shown in Figure 1) were initially identified within a spectrum recorded over 7.0–18.5 GHz while using argon as the carrier gas and were then observed again during experiments performed using neon carrier gas. No transitions of other conformers were identified while using either argon or neon. Microwave spectroscopy experiments performed using argon typically isolate those conformers (typically only 1 or 2 different conformational forms) that have the lowest energy.[29] It is sometimes possible to observe a greater number of conformers, including higher-energy conformers, through experiments that use a neon carrier gas.[30] However, microwave spectroscopy experiments which probe very cold molecules and complexes will always tend to detect low-energy conformers in higher abundance than higher-energy conformers. The quantum chemical calculations of the present work support that the geometry pictured in Figure 1 is the lowest-energy conformer of 2-ET.

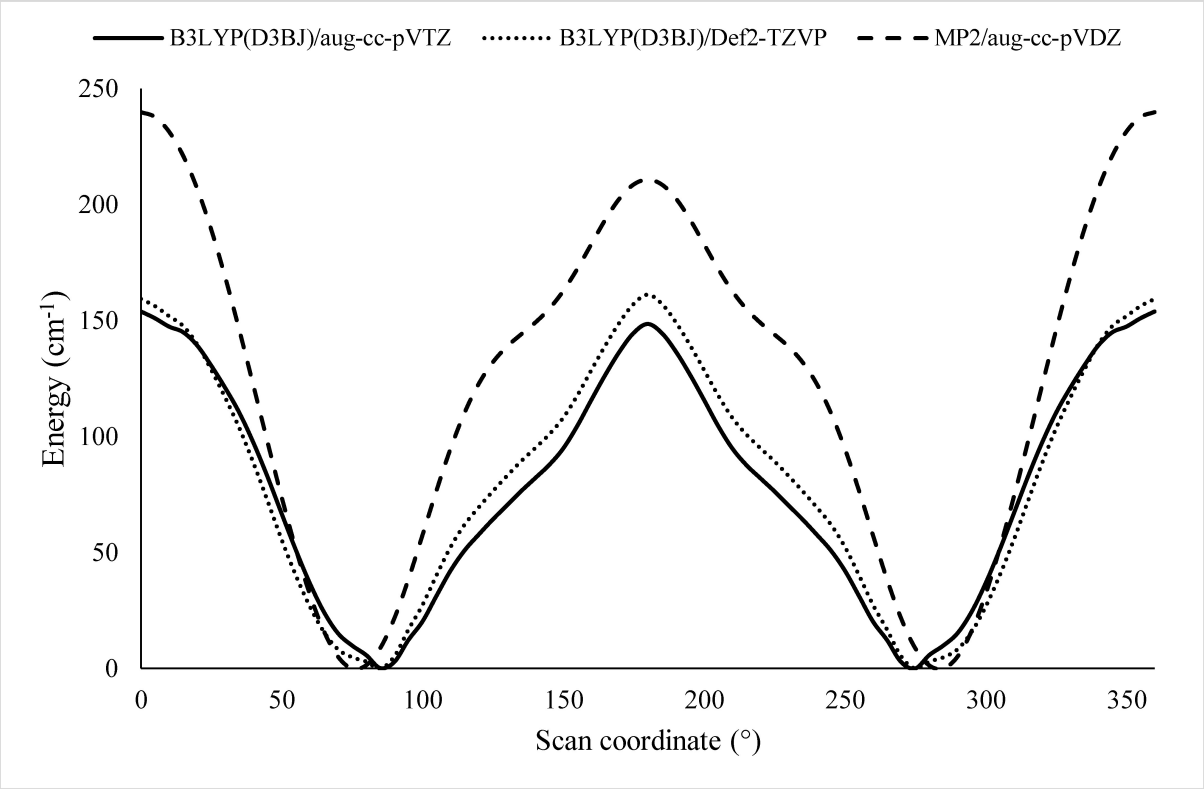

Figure 2. Potential energy scans obtained by rotating the ethyl group relative to the thiazole ring in 2-ET. Calculations performed at the B3LYP(D3BJ)/aug-cc-pVTZ, B3LYP(D3BJ)/Def2-TZVP and MP2/aug-cc-pVDZ levels of theory by scanning the ∠(C7-C6-C2-N) dihedral angle (atom labelling given in Figure 1).

The spectrum of the isolated 2-ET molecule was assigned by fitting experimentally-observed transitions to parameters in Watson's *S*-reduced Hamiltonian.[31] Each transition exhibited hyperfine structure owing to the presence of a nitrogen nucleus. In total, 180 hyperfine components were assigned across the 2–18.5 GHz frequency region. Within the spectrum, *a*-, *b*- and *c*-type transitions were observed for 2-ET, as expected, since the results of calculations performed at several different levels of theory predict a non-zero dipole moment component along each axis. The observation of *c*-type transitions within the spectrum indicates that mass lies outside of the *ab* plane confirming that the conformer identified is non-planar. The spectrum was initially assigned to the global minimum structure identified by quantum chemical calculations based on good agreement between the experimentally-determined spectroscopic constants and the equilibrium rotational constants presented in Table S1. Details of the Hamiltonian and parameters employed by the spectroscopic fits are provided below.

The microwave spectra of one ^{34}S-containing and five ^{13}C-containing isotopologues were readily assigned within the spectrum recorded for a 2-ET sample with isotopes in their naturally-occurring abundances. The naturally-occurring isotopic abundance ratios of ^{34}S and ^{13}C are respectively 4.25% and 1.07%. The spectrum of each singly-substituted isotopologue was assigned and fitted to determine rotational constants (A_0, B_0 and C_0) while centrifugal distortion and nuclear quadrupole coupling constants were held fixed at the values determined for the parent isotopologue. The results of the fits performed for lower-abundance isotopologues of 2-ET are displayed in Table S16. Quantum chemical calculations found (as shown in Table S1) that the projection of the dipole moment onto the *b*-inertial axis, μ_b, is significantly greater than the projections onto the *a*- and *c*- inertial axes which are denoted by μ_a and μ_c. Therefore, it is unsurprising that only *b*-type transitions were observed for the spectra of singly-substituted isotopologues. The naturally-occurring isotopic abundance ratio of ^{15}N is 0.4%. The spectrum of the most abundant ^{15}N-containing isotopologue was sought but not identified nor assigned, presumably because its concentration is too low for detection at the sensitivity of the present experiments.

After assigning transitions of the isolated 2-ET molecule, many transitions remained unassigned within the spectra recorded over the 7.0–18.5 GHz and 2–8 GHz ranges. Given the experimental method employed, it was anticipated that transitions may assign to complexes formed between one or more H_2O molecules and 2-ET. Both the binary complex formed between 2-ET and H_2O and the ternary complex formed between 2-ET and two H_2O molecules were calculated to be near-prolate asymmetric tops with μ_a being greater than μ_b or μ_c. A tentative, preliminary assignment of the spectrum of 2-ET···$H_2{}^{16}O$ assumed the geometry calculated for the lowest-energy conformer of this complex and found good agreement between experimentally-determined and DFT-calculated spectroscopic constants. The 2-ET sub-unit has C_1 symmetry (similar to that observed for the isolated 2-ET molecule) within the geometry of this complex. A total of 158 hyperfine components were assigned to the

spectrum of 2-ET···$H_2{}^{16}O$ and fitted using Watson's *S*-reduced Hamiltonian. The spectrum of the complex proved sufficiently intense to allow the observation and assignment of transitions of the ^{34}S-containing isotopologue which confirmed the geometry to be as calculated for the lowest-energy conformer shown in Figure 1. Consistent with the calculated values of μ_a, μ_b and μ_c, only *a*-type transitions were assigned for both ^{32}S-containing and ^{34}S-containing isotopologues of 2-ET···$H_2{}^{16}O$. Consistent with the previous studies[3,4] of thiazole···H_2O, 4-methylthiazole···H_2O and 5-methylthiazole···H_2O, transitions of only a single conformer of 2-ET···H_2O were assigned under the experimental conditions employed. Given the small splittings caused by nuclear quadrupole coupling of the nitrogen atom, multiplets of hyperfine components in the spectra of both 2-ET and 2-ET···H_2O were sometimes observed as blended features preventing the identification of accurate transition centre frequencies. This effect reduces the precision with which spectroscopic parameters can be determined which is reflected in the uncertainties quoted.

A previous study identified two isomers of thiazole···$(H_2O)_2$ which were denoted as isomers I and II (where isomer I is the lowest-energy conformer).[11] An oxygen atom was observed to form a weak interaction with the H atom on C2 (atom numbering is the same as that presented in Figure 1) in isomer I whereas the interaction is with the H atom at C4 in isomer II. The quantum chemical calculations of the present work found that the geometry shown in Figure 1 is the lowest-energy conformer of 2-ET···$(H_2O)_2$. Within this geometry, the intermolecular binding interaction between $(H_2O)_2$ and the thiazole ring is similar to that found in isomer I of thiazole···$(H_2O)_2$. A preliminary assignment of the spectrum of this conformer of 2-ET···$(H_2{}^{16}O)_2$ was made on basis of the rotational constants calculated for the geometry of this complex as shown in Figure 1. Intense *a*-type transitions and weaker *b*-type transitions were identified. The relative intensities are consistent with expectations based on the relative magnitudes calculated for μ_a and μ_b. Across the 2–18.5 GHz frequency region, a total of 182 transitions were assigned and fitted for this isomer. A search for transitions was performed but did not yield evidence of further higher-energy isomers. The calculated difference in energy between the two lowest-energy conformers of 2-ET···$(H_2{}^{16}O)_2$ is predicted to be 1.8 kJ mol^{-1} at the B3LYP(D3BJ)/aug-cc-pVTZ level of theory whereas the difference in energy between the two lowest-energy conformers of thiazole···$(H_2O)_2$ was reported to be 3.5 kJ mol^{-1} at the same level of theory. To verify the assignments of all the spectra assigned to hydrates of 2-ET during this work, experiments were performed using isotopically-enriched samples of $H_2{}^{18}O$ and D_2O. These samples ultimately allowed for assignment and fitting of the spectra of 2-ET···$H_2{}^{18}O$, 2-ET···DOH, 2-ET···HOD and 2-ET···D_2O isotopologues for the monohydrate; and of the spectra of 2-ET···$(H_2{}^{18}O)(H_2{}^{16}O)$ and 2-ET···$(H_2{}^{16}O)(H_2{}^{18}O)$ for the dihydrate.

For each of 2-ET, 2-ET···H_2O and 2-ET···$(H_2O)_2$, the measured frequencies of transitions in the spectra were assigned and fits performed to determine parameters in Watson's *S*-reduced Hamiltonian[31] using Western's PGOPHER[32] program;

$$H = H_R - \frac{1}{6}\mathrm{Q(14N)} : \nabla \mathrm{E(14N)} \quad (1)$$

where H_R is the energy operator for a semi-rigid asymmetric rotor which has contributions from rotational constants (A_0, B_0 and C_0) and centrifugal distortion constants (D_J, D_{JK}, D_K, d_1 and d_2). The presence of the nitrogen nucleus ($I=1$ for ^{14}N) within the thiazole ring leads to hyperfine structure in the spectra of each of the species identified, as shown in Figure 3. The second term within Equation (1) models the interaction between the nuclear electric quadrupole moment, $Q(^{14}N)$, and the electric field gradient, $\nabla E(^{14}N)$, at the nitrogen nucleus. Matrix elements were constructed in the ($I_N + J = F$) basis and diagonalised in blocks of the quantum number, *F*. For the isolated 2-ET molecule, rotational constants, centrifugal distortion constants and nuclear quadrupole coupling constants (χ_{aa}(N) and [χ_{bb}(N)–χ_{cc}(N)]) were determined for the parent isotopologue as shown in Table 1. Fits of the spectra of other isotopologues assumed values of centrifugal distortion and nuclear quadrupole coupling constants which were equal to those determined for the parent. For 2-ET···H_2O, rotational constants, centrifugal distortion constants and χ_{aa}(N) were determined by fitting for all isotopologues studied (Table 2). The value of [χ_{bb}(N)–χ_{cc}(N)] was fixed at the result determined for the parent isotopologue in the fits performed for 2-ET···$H_2{}^{18}O$, 2-ET···DOH and 2-ET···HOD, 2-ET···D_2O and for the ^{34}S-containing isotopologue. Transitions in the spectrum of 2-ET···$(H_2{}^{16}O)_2$ were fitted to determine the rotational constants, centrifugal distortion constants and the nuclear quadrupole coupling constants (χ_{aa}(N) and [χ_{bb}(N)–χ_{cc}(N)]). Isotopic "scrambling" on introduction of $H_2{}^{18}O$ into the chemical sample meant

Table 1. Spectroscopic parameters determined for the parent isotopologue of 2-ET by fitting experimentally-recorded transition frequencies to parameters in Watson's *S*-reduced Hamiltonian.

Parameter	2-ET
A_0 (MHz)	4457.00890(69)[a]
B_0 (MHz)	1758.06359(34)
C_0 (MHz)	1387.24304(30)
D_J (kHz)	0.5075(52)
D_{JK} (kHz)	19.280(16)
D_K (kHz)	−16.603(77)
d_1 (kHz)	0.0038(15)
d_2 (kHz)	0.05038(62)
χ_{aa} (N) (MHz)	0.3284(45)
[χ_{bb}(N)–χ_{cc}(N)] (MHz)	−4.7707(65)
σ_{rms} (kHz)[b]	9.0
N[c]	180
a/*b*/*c*[d]	y/y/y
P_{cc} (u Å^2)	18.27429(5)

[a] Numbers in parentheses are one standard deviation in units of the last significant figure. [b] Root mean square (rms) deviation of the fit. [c] Number of hyperfine components included in the fit. [d] "y" indicates that this type of transition was observed.

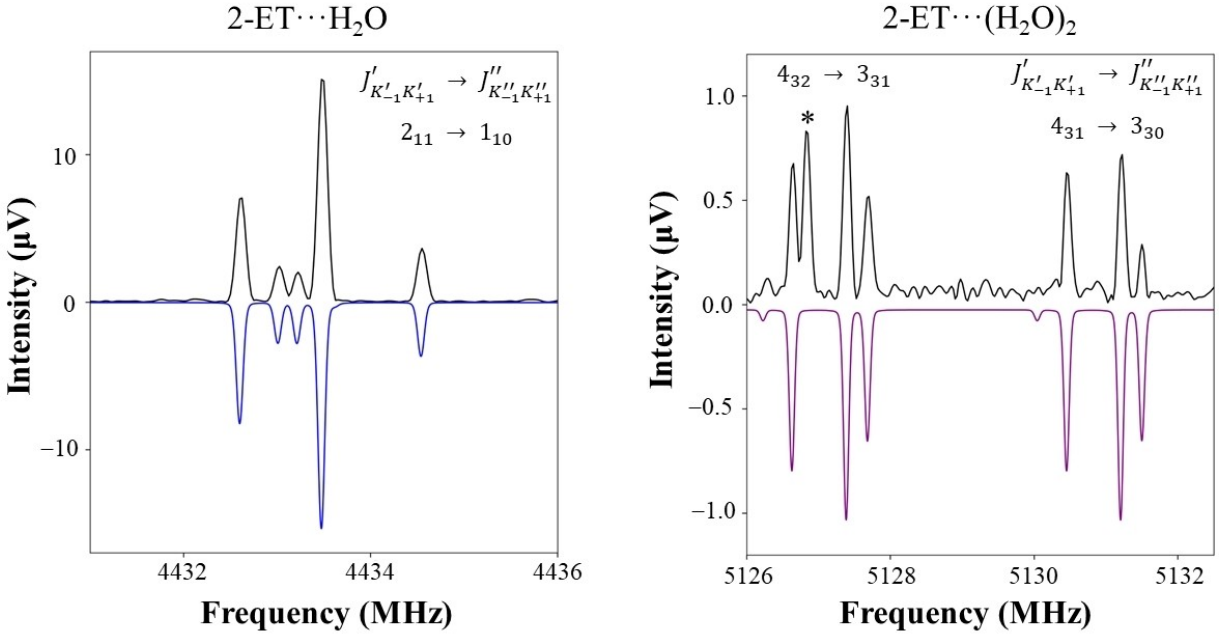

Figure 3. (left) $2_{11}\rightarrow1_{10}$ rotational transition of 2-ET···$H_2{}^{16}O$. (right) $4_{32}\rightarrow3_{31}$ and $4_{31}\rightarrow3_{30}$ rotational transitions of 2-ET···$(H_2{}^{16}O)_2$. The experimental spectrum (black trace) recorded while probing a sample containing 2-ET and $H_2{}^{16}O$ in neon carrier gas is displayed above a simulation (blue and purple) prepared using PGOPHER. The transition labeled with an asterisk is assigned to the ^{34}S isotopologue of 2-ET.

Table 2. Experimentally-determined spectroscopic parameters for six isotopologues of 2-ET···H_2O.

	$H_2{}^{16}O$	$^{34}S1$	$H_2{}^{18}O$	DOH	HOD	D_2O
A_0 (MHz)	2334.3770(12)[a]	2324.477(15)	2303.7980(68)	2314.9159(69)	2295.6969(83)	2278.7560(70)
B_0 (MHz)	1195.92729(35)	1178.9223(14)	1143.55402(69)	1184.02980(74)	1162.20114(53)	1150.80772(83)
C_0 (MHz)	845.54396(28)	835.8513(12)	815.32658(70)	837.04353(65)	823.88092(65)	815.97858(72)
D_J (kHz)	0.2274(21)	0.2424(91)	0.2120(26)	0.2097(69)	0.2302(43)	0.1911(44)
D_{JK} (kHz)	0.446(13)	0.39(15)	0.740(26)	0.632(89)	0.432(57)	0.631(41)
d_1 (kHz)	−0.0704(13)	−0.0770(65)	−0.0474(23)	−0.0646(39)	[−0.0704][b]	−0.0520(32)
χ_{aa} (N) (MHz)	−2.8552(82)	−2.899(22)	−2.9841(87)	−2.888(13)	−2.962(11)	−3.038(14)
$[\chi_{bb}(N)-\chi_{cc}(N)]$ (MHz)	−1.225(19)	[−1.225]	[−1.225]	[−1.225]	[−1.225]	[−1.225]
σ_{rms} (kHz)[c]	11.7	16.0	11.9	15.2	13.7	12.0
N[d]	158	68	125	88	84	97
P_{cc} (u Å^2)	20.69033(13)	20.7336(9)	20.7282(4)	20.6886(4)	20.7878(5)	20.7884(5)

[a] Numbers in parentheses are one standard deviation in units of the last significant figure. [b] Values in square brackets held fixed at the result for the parent isotopologue, 2-ET···$H_2{}^{16}O$. [c] Root mean square (rms) deviation of the fit. [d] Number of hyperfine components included in the fit.

that the abundance of each of the ^{18}O-containing isotopologues (and hence the S/N of measured transitions) was unavoidably lower than was achieved for the parent isotopologue, 2-ET···$(H_2{}^{16}O)_2$. Hence, the fits performed for each of 2-ET···$(H_2{}^{18}O)(H_2{}^{16}O)$ and 2-ET···$(H_2{}^{16}O)(H_2{}^{18}O)$ assumed the values of D_{JK}, d_1, d_2 and $[\chi_{bb}(N)-\chi_{cc}(N)]$ determined for the parent isotopologue (Table 3). Transitions included in fits of the data for these isotopologues were recorded in the 2–8 GHz band because transitions observed in the 7.0–18.5 GHz band were observed to have significantly lower S/N. Diagonalisation of the nuclear quadrupole coupling tensor followed by transformation into the framework of principal nuclear axes at the nitrogen atom (using the QDIAG program) allowed $\chi_{xx}(N)$, $\chi_{yy}(N)$ and $\chi_{zz}(N)$ to be determined for the parent isotopologue of each of 2-ET, 2-ET···H_2O and 2-ET···$(H_2O)_2$, allowing direct comparison with the same constants calculated for the thiazole monomer.[33] The off-diagonal term, χ_{ab}, used in each calculation was chosen to be consistent with the value calculated at the B3LYP(D3BJ)/aug-cc-

Table 3. Experimentally-determined spectroscopic parameters for three isotopologues of 2-ET···$(H_2O)_2$.

	$(H_2{}^{16}O)_2$	$(H_2{}^{18}O)$ $(H_2{}^{16}O)$	$(H_2{}^{16}O)$ $(H_2{}^{18}O)$
A_0 (MHz)	1911.5874(23)[a]	1864.280(55)	1901.6656(82)
B_0 (MHz)	709.82247(45)	698.6077(16)	682.2168(14)
C_0 (MHz)	566.38146(36)	555.2502(13)	549.0672(15)
D_J (kHz)	0.20916(90)	0.211(18)	0.159(27)
D_{JK} (kHz)	−0.9039(65)	[−0.9039][b]	[−0.9039]
d_1 (kHz)	−0.0211(10)	[−0.0211]	[−0.0211]
d_2 (kHz)	−0.00400(56)	[−0.004]	[−0.004]
χ_{aa}(N) (MHz)	−2.5687(93)	−2.668(23)	−2.533(27)
$[\chi_{bb}(N)-\chi_{cc}(N)]$ (MHz)	−1.261(44)	[−1.261]	[−1.261]
σ_{rms} (kHz)[c]	11.0	15.4	14.6
N[d]	182	38	30
P_{cc} (u Å^2)	42.0308(4)	42.156(4)	43.0567(16)

[a] Numbers in parentheses are one standard deviation in units of the last significant figure. [b] Values in square brackets held fixed at the result for the parent isotopologue, 2-ET···$(H_2{}^{16}O)_2$. [c] Root mean square (rms) deviation of the fit. [d] Number of hyperfine components included in the fit.

pVTZ level for each species. The values obtained, displayed in Table S17, are slightly lower than the values previously reported for thiazole. Observed transition frequencies of each isotopologue of 2-ET, 2-ET···H_2O and 2-ET···$(H_2O)_2$ are provided in Tables S18-S33.

Molecular Geometry

The spectrum of the observed conformer of 2-ethylthiazole was initially assigned on basis of good agreement between the rotational constants determined experimentally and those which were calculated for the geometry shown in Figure 1. Observation of *a*-, *b*- and *c*-type transitions confirmed that the observed conformer is non-planar and has C_1 symmetry. Quantities calculated from the experimentally-determined rotational constants provide further evidence in support of the geometry shown in Figure 1. The values of inertial defects, Δ_0, determined for thiazole[34] and 2-methylthiazole[35,36] by previous works are respectively 0.0744(4) u Å^2 and −3.0828(12) u Å^2. The small and positive result for thiazole is consistent with a planar geometry. The result for 2-methylthiazole reflects that a small amount of out-of-plane mass is contributed by the three hydrogen atoms of the CH_3 group. The inertial defect of the isolated 2-ET molecule is calculated from the experimentally-determined moments of inertia about the *a*, *b* and *c* inertial axes as follows;

$$\Delta_0 = I_{cc}\text{-}I_{bb}\text{-}I_{aa} \quad (2)$$

and determined to be −36.54857(10) u Å^2. This result is significantly larger than those of each of thiazole and 2-methylthiazole and consistent with the non-planar geometry shown in Figure 1. The planar moment, P_{cc}, of 2-ET can be directly calculated from the inertial defect using $P_{cc} = \sum m_i c_i^2 = -\Delta_0/2$ and is 18.27429(5) u Å^2. This result requires that one or more heavy atoms is significantly displaced from the *ab* plane.

The availability of rotational constants for seven isotopologues of 2-ET allows the determination of substitution (r_s) coordinates for all of the C and S atoms within the molecule using Kraitchman's equations implemented within KRA[37] (available on the PROSPE website). The resulting coordinates and their Costain errors[38] are displayed in Table S34 alongside equilibrium (r_e) coordinates for each atom calculated at the ωB97X-D/aug-cc-pVQZ level of theory. The method determines only the magnitude of each coordinate, the correct signs are inferred from the r_e coordinates. An imaginary *c*-coordinate was obtained for the sulfur atom indicating that it lies within the *ab* plane (at the precision of the experiments) whereas the *c*-coordinates for all other atoms are non-zero. It is not possible to determine values of all internal coordinates because of the lack of information regarding the position of the nitrogen atom but the values of some bond lengths, bond angles and dihedral angles have been derived (Table S35) using EVAL. It is interesting to note the degree of rotation of the ethyl group relative to the thiazole ring which is represented by ∠(C7-C6-C2-S) and calculated to be −98.6(10)° from the r_s coordinates. The quantum chemical calculations imply some variation in the calculated value of this angle across the different levels of theory used. At the ωB97X-D/aug-cc-pVQZ it is calculated to be −110.3° whereas it is calculated to be −97.9° at the B3LYP(D3BJ)/Def2-TZVP level which is in better agreement with the experimentally-determined (r_s) result. There is an angle of 12.6° between the horizontal plane of symmetry of the thiazole ring sub-unit and the *ab* plane of the molecule in the model (ωB97X-D/aug-cc-pVQZ calculated, r_e) geometry of 2-ET shown in Figure 1.

Spectra of $H_2{}^{18}O$-containing isotopologues were recorded for each of 2-ET···H_2O and 2-ET···$(H_2O)_2$ to verify the assignment of the spectrum to the correct molecular carrier and inform the determination of structural parameters. The spectra of deuterated isotopologues were recorded for the monohydrate allowing more detailed structural interpretation for that complex. Before reporting on evaluated bond lengths and angles, it is first interesting to note some implications of the determined planar moments, P_{cc}, for 2-ET···H_2O and 2-ET···$(H_2O)_2$. The result for P_{cc} of 2-ET···$H_2{}^{16}O$ is 20.69033(13) u Å^2 which reflects that 2-ET···$H_2{}^{16}O$ has more out-of-(*ab*)plane mass than does the isolated 2-ET molecule for which P_{cc} = 18.27429(5) u Å^2 as noted above. Results reported previously show that contributions of the H_2O sub-unit to P_{cc} of 4-methylthiazole···H_2O and 5-methylthiazole···H_2O are of the order of 0.5 u Å^2 and 0.2 u Å^2 respectively.[4] These contributions were attributed to zero-point vibrational motion affecting the non-bonding hydrogen atom, H_{nb}, in each complex. Evidently, the contribution of the H_2O sub-unit to P_{cc} for 2-ET is of the order of 2.4 u Å^2. This is somewhat too large to be rationalised by the zero-point vibrational motions alone and will be discussed further below. The P_{cc} of 2-ET···$(H_2{}^{16}O)_2$ is 42.0308(4) u Å^2 which is significantly greater than the P_{cc} of each of 2-ET···H_2O and 2-ET···$(H_2O)_2$ and requires that a larger fraction of the

mass of the H_2O molecules is out-of-(*ab*)plane in 2-ET···$(H_2O)_2$. There is only small variation of P_{cc} across the range of isotopologues of each of these complexes as shown in Tables 2 and 3.

The results available for isotopologues of 2-ET···H_2O allow the determination of r_s coordinates presented in Table 4 for the bonding hydrogen atom, H_b, the oxygen atom, O, and for H_{nb}. The experimentally-determined r_s and ωB97X-D/aug-cc-pVQZ calculated r_e coordinates generally show good agreement with some minor differences observed in the coordinates of the H_{nb} atom. Minor differences between r_s and r_e results are expected because the experiment probes the complex in the vibrational ground state whereas the calculations are for the equilibrium geometry of the complex. The H_{nb} atom undergoes rapid zero-point motions which lead to uncertainties in the *c*-coordinate of this atom and differences between r_s, r_0 and r_e results. The small but non-zero r_s coordinate for the oxygen atom confirms that it is slightly displaced from the *ab* plane of the complex such that it significantly contributes to P_{cc}. The ∠(O···N-C2-S) dihedral angle is 177.0(2)° if the experimentally-determined r_s coordinates of O are used alongside the ωB97X-D/aug-cc-pVQZ calculated r_e coordinates of the N, C2 and S atoms in the calculation of this internal coordinate. Assignment of the spectrum of an ^{34}S-containing isotopologue of 2-ET···$H_2{}^{16}O$ allowed determination of the substitution coordinates of the sulphur atom as −1.75076(87), −0.6783(22) and −0.150(10) Å which compare with the r_e coordinates, −1.758, −0.677 and −0.129 Å calculated at the ωB97X-D/aug-cc-pVQZ level of theory.

To gain deeper insight into the intermolecular interactions present, ground-state (r_0) structural parameters were determined for 2-ET···H_2O using Kisiel's STRFIT program.[39] In order to perform the r_0 fit, geometrical parameters internal to each of the sub-units, 2-ET and H_2O, were assumed equal to their r_e values calculated at the ωB97X-D/aug-cc-pVQZ level of theory. The r_0 fits of previous works[3,11,4] which studied thiazole···H_2O, thiazole···$(H_2O)_2$ and 5-methylthiazole···H_2O complexes assumed that the dihedral angles, ∠(O···N-C2-S), ∠(H_b-O···N-C2) and ∠(H_{nb}-O-H_b···N), are equal to 180°. Atoms which are internal to the H_2O molecule were thus fixed to lie within the plane of the thiazole ring to represent an average over zero-point vibrational motions. Noting the difference of 2.4 u Å^2 between P_{cc} for the isolated 2-ET molecule and for the 2-ET···H_2O complex, and the non-zero r_s coordinate of oxygen which confirms that it is slightly displaced from the *ab* plane in 2-ET···H_2O, different assumptions were made during the present work. It was assumed that ∠(O···N-C2-S) and ∠(H_b-O···N-C2) are equal to the ωB97X-D/aug-cc-pVQZ calculated (r_e) results of 176.8° and 169.9° respectively when fitting r_0 parameters. These assumptions lead to good agreement between fitted r_0 and calculated r_e results for *r*(O···N), ∠(O···N-C2) and ∠(H_b-O···N) as shown in Table 5. The good agreement between r_0 and r_e parameters is perhaps surprising. 2-ET has lower symmetry and a greater number of internal vibrational coordinates than do thiazole, 4-methylthiazole or 5-methylthiazole which implies that the assumed values of parameters may approximate zero-point motions less well for 2-ET···H_2O than for the other complexes. The P_{cc} implied by the ωB97X-D/aug-cc-pVQZ calculated geometries of 2-ET and 2-ET···H_2O are 16.4 u Å^2 and 20.0 u Å^2 respectively which are slightly different from those obtained from the experimentally-determined spectroscopic parameters (18.27429(5) u Å^2 and 20.69033(13) u Å^2 respectively). Nevertheless, the results are consistent with the binding geometries and the overall trend identified previously.[4] A comparatively strong hydrogen bond is present between the O–H bond

Table 4. Comparison of experimentally-determined (r_s) and DFT-calculated (r_e) atomic coordinates of H_b, O, H_{nb} and S in 2-ET···H_2O and O1, O2 atoms in 2-ET···$(H_2O)_2$.

2-ET···H_2O				
	Method	*a*/Å	*b*/Å	*c*/Å
H_b	r_e (calc.)[a]	2.1026	1.3232	−0.0913
	r_s (exp.)	2.05337(74)[b]	1.3645(11)	[0][c]
O	r_e (calc.)	3.0720	1.2903	−0.1282
	r_s (exp.)	3.10633(48)	1.2533(12)	−0.143(11)
H_{nb}	r_e (calc.)	3.3434	2.1123	−0.5309
	r_s (exp.)	3.45971(44)	1.93983(78)	−0.3206(48)
S	r_e (calc.)	−1.7584	−0.6770	−0.1293
	r_s (exp.)	−1.75076(87)	−0.6783(22)	−0.150(10)
2-ET···$(H_2O)_2$				
	Method	*a*/Å	*b*/Å	*c*/Å
O1	r_e (calc.)[a]	2.3485	1.8052	0.3492
	r_s (exp.)	2.37294(77)	1.8468(10)	0.2583(72)
O2	r_e (calc.)	3.7194	−0.3532	−0.8088
	r_s (exp.)	3.74366(42)	−0.4345(36)	−0.7367(21)

[a] r_e geometry calculated at the ωB97X-D/aug-cc-pVQZ level of theory. [b] Numbers in parentheses after r_s results are Costain errors calculated as $\delta a = 0.015/|a|$. [c] Imaginary r_s coordinate was obtained ($r_s(H_b) = 0.042i(36)$) so its value is assumed equal to zero.

Table 5. Comparison of DFT-calculated (r_e) and experimentally-determined (r_0) structural parameters for 2-ET···H_2O.

Parameter	Method	Value
r(O···N)/Å	r_e (calc.) [a]	2.893
	r_0 (exp.)	2.9257(48)[b]
∠(O···N-C2)/°	r_e (calc.)	109.1
	r_0 (exp.)	109.726(91)
∠(H_b-O···N)/°	r_e (calc.)	9.1
	r_0 (exp.)	11.3(36)
r(H_b···N)/Å	r_e (calc.)	1.940
	r_0 (exp., derived)[c]	1.983(13)
∠(H_b···N-C2)/°	r_e (calc.)	113.6
	r_0 (exp., derived)	115.1(17)
∠(O-H_b···N)/°	r_e (calc.)	166.3
	r_0 (exp., derived)	163.3(52)

[a] r_e geometry calculated at the ωB97X-D/aug-cc-pVQZ level of theory. [b] Numbers in parentheses are one standard deviation in units of the last significant figure. [c] *r*(O···N), ∠(O···N-C2) and ∠(H_b-O···N) determined by fitting to the experimentally-determined rotational constants. Results for other parameters derived from the atomic coordinates using the EVAL program.

of H_2O and the nitrogen atom. This hydrogen bond is somewhat non-linear, as evidenced by ∠(O-H_b ···N) = 163.3(52)°, implying the presence of a weak, additional hydrogen-bonding interaction between the O atom and the ethyl group substituent on the 2-position of the ring. This possibility will be examined further in the Discussion. It was found that the oxygen atom is co-planar with the heteroaromatic ring (which is itself co-planar with the *ab* plane of each complex) in each of *N*-methylimidazole···H_2O, 2-methylimidazole···H_2O, 4-methylthiazole···H_2O and 5-methylthiazole···H_2O.[2,4] The orientation of the ethyl group has a small but significant effect on the position of the oxygen atom within 2-ET···H_2O. The angle between the *ab* plane and the horizontal symmetry plane of the thiazole ring sub-unit is 13.3° for the complex (in the ωB97X-D/aug-cc-pVQZ calculated, r_e geometry). While the oxygen atom is slightly displaced from the *ab* plane (the *c*-coordinate (r_s) is −0.143(11) Å), it is also slightly displaced from the symmetry plane of the thiazole ring sub-unit, by 0.150(1) Å, when this distance is calculated from the r_0 coordinate of the O atom given in Table 5 and the orientation of the plane implied by the calculated r_e coordinates of atoms within the thiazole ring sub-unit.

The range of isotopologues of 2-ET···$(H_2O)_2$ studied was narrower than achieved for 2-ET···H_2O. Recording of the spectra of both 2-ET···$(H_2{}^{18}O)(H_2{}^{16}O)$ isotopomers and the 2-ET···$(H_2{}^{16}O)_2$ parent allowed for r_s coordinates of the oxygen atoms to be determined as shown in Table 4 implying a distance between the O atoms, *r*(O1···O2), of 2.8413(40) Å. Spectra were not recorded for deuterated isotopologues of 2-ET···$(H_2O)_2$ precluding the direct determination of structural parameters which depend on hydrogen atom atomic coordinates. A fit performed under the assumption that all atoms of both H_2O molecules lie within the horizontal symmetry plane of the thiazole ring yielded a high standard deviation. This is unsurprising because the evaluated P_{cc} for 2-ET···$(H_2O)_2$ already provide a clear indication that a large fraction of the mass of the two H_2O sub-units lies outside the *ab* plane of the complex and the r_s coordinate of O2 (Table 4) was determined to be −0.7367(21) Å. Under the alternative assumption that in-plane and dihedral angles which define the orientations of hydrogen atoms (relative to the positions of the heavy atoms) are equal to r_e calculated results (ωB97X-D/aug-cc-pVQZ), two interatomic distances (*r*(O1···N) and *r*(O1···O2)) and the ∠(O1···N-C2) angle were determined by the r_0 method and found to be highly-consistent with the r_e calculated results as shown in Table 6. The internal geometries of the 2-ET and H_2O sub-units were assumed equal to the calculated (ωB97X-D/aug-cc-pVQZ, r_e) results when this fit was performed. It is interesting to compare the values obtained for the *r*(O1···N) and ∠(O1···N-C2) structural parameters for the mono- and dihydrate complexes. Comparing the r_0 parameters, the *r*(O···N) distance is 2.9307(30) Å in the monohydrate but only 2.8235(72) Å in the dihydrate. The ∠(O1···N-C2) angle is 108.902(51)° in the monohydrate but 120.55(15)° in the dihydrate. The *r*(O1···O2) distance within the dihydrate is determined to be 2.894(21) Å which is in good agreement with the r_s result mentioned earlier and the r_e result of 2.807 Å. Atomic coordinates calculated as described for 2-ET···H_2O and 2-ET···$(H_2O)_2$ are presented in Tables S36–S38.

Table 6. Comparison of DFT-calculated (r_e) and experimentally-determined (r_0) structural parameters of 2-ET···$(H_2O)_2$.

Parameter	Method	Value
r(O1···N)/Å	r_e (calc.)[a]	2.827
	r_0 (exp.)	2.8235(72)[b]
r(O1···O2)/Å	r_e (calc.)	2.807
	r_0 (exp.)	2.894(21)
∠(O1···N-C2) /°	r_e (calc.)	118.4
	r_0 (exp.)	120.55(15)

[a] r_e geometry calculated at the ωB97X-D/aug-cc-pVQZ level of theory.[b] Numbers in parentheses are one standard deviation in units of the last significant figure.

Non-Covalent Interactions

Non-Covalent Interactions (NCI)[40] and Natural Bond Orbital (NBO)[41] analyses were performed to provide an insight into the intermolecular interactions present within each of 2-ET···H_2O and 2-ET···$(H_2O)_2$. The geometries of the complexes calculated at the ωB97X-D/aug-cc-pVQZ level of theory were used by the analysis. NCI plots of the reduced density gradient, RDG, versus the sign of the second eigenvalue of the Hessian matrix (λ_2) of the electronic density (ρ), sign(λ_2)ρ, were generated using the program Multiwfn[42] and are displayed in Figure 4. The results of the analysis confirm that each of 2-ET and water simultaneously acts as a hydrogen bond donor and acceptor within each complex. For the 2-ET···H_2O complex, a dark blue isosurface is located between the nitrogen atom on the thiazole ring and one of the H atoms of the water molecule, indicating the presence of a strong attractive hydrogen bonding interaction. A second larger isosurface is present between the O atom of the water molecule and the ethyl group and shows weakly attractive (light green, negative sign(λ_2)ρ) and weakly repulsive interactions (dark green, positive sign(λ_2)ρ). Weakly attractive interactions are located between the O atom and the nearest H atoms located on both C6 and C7. The NCI analysis of 2-ET···$(H_2O)_2$ revealed the presence of two dark blue isosurfaces within this complex. In addition to the isosurface indicating the interaction between N and the hydrogen atom (H_{1b}) on the first water molecule, another relatively strong hydrogen bonding interaction is present between O1 of the first water molecule and one of the H atoms, H_{2b}, on the second water molecule. There is also a weak attractive interaction between the O atom of O2 and an H atom on C6 of the ethyl group.

NBO analysis was performed at the B3LYP(D3BJ)/aug-cc-pVTZ level of theory using the geometries of the complexes calculated at the ωB97X-D/aug-cc-pVQZ level which calculates the second order stabilisation energies ($E^{(2)}$) of each interaction present. The results of the NBO analysis are displayed in the supplementary information, Tables S39 and S40. In the 2-ET···H_2O complex, the largest $E^{(2)}$ is for an interaction between the lone pair of the N atom and the σ*(H_b-O) orbital of the water molecule. This interaction has a second order stabilisation energy of 40.67 kJ mol^{-1}, which is very similar to the values obtained for

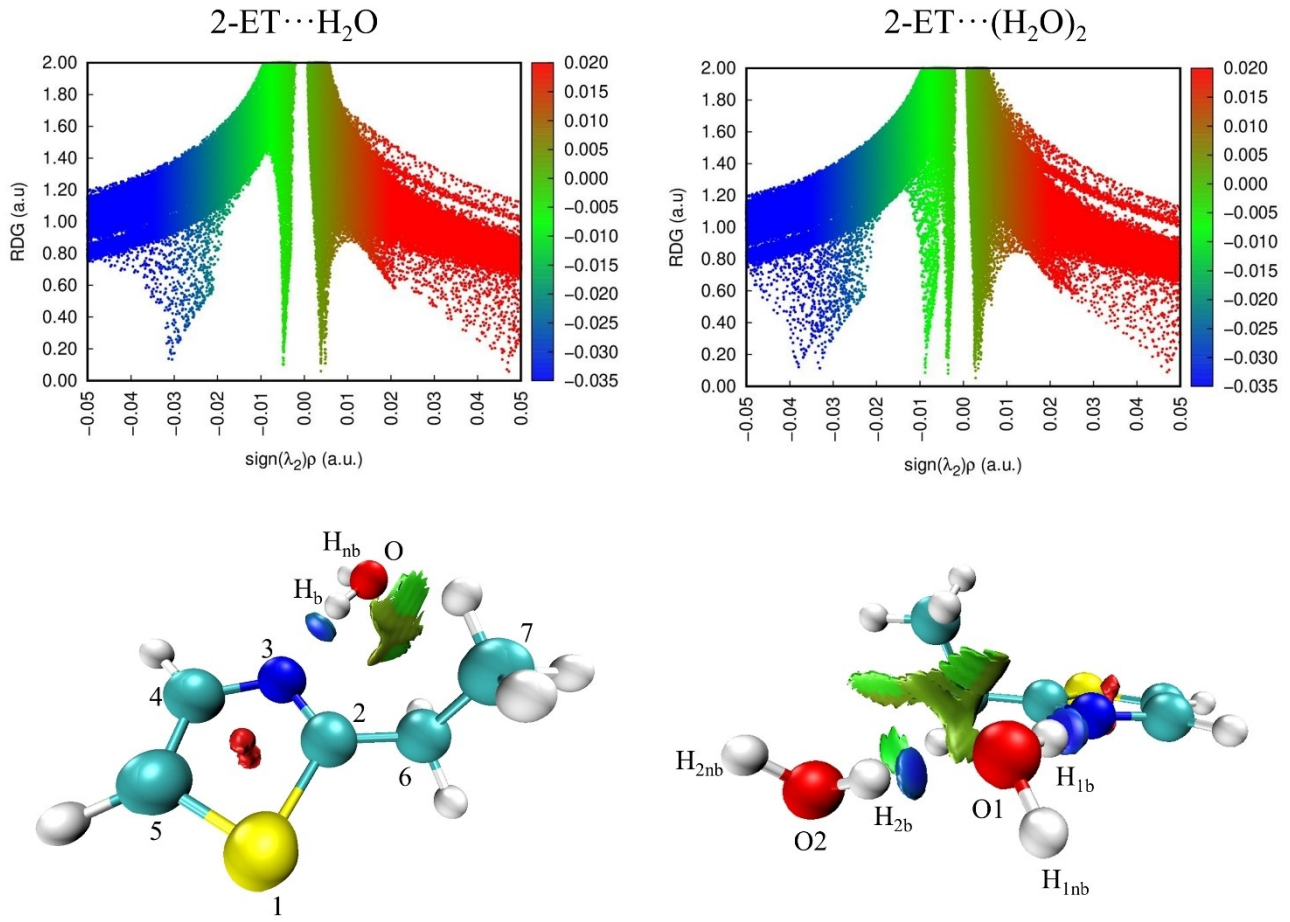

Figure 4. NCI isosurfaces and plots of the RDG (a.u.) vs sign(λ_2)ρ of 2-ET···H_2O and 2-ET···$(H_2O)_2$. Positive and negative values of sign (λ_2)ρ respectively denote repulsive (red) and attractive (blue) interactions. The isosurface s value is 0.5 au.

the equivalent interactions in the thiazole···H_2O, 4-methylthiazole···H_2O and 5-methylthiazole···H_2O complexes.[3,4] The NBO analysis also revealed additional weaker interactions between the O atom of the water molecule and hydrogen atoms of the ethyl group. The lone pairs on the O atom form an interaction with the nearest H atoms located on C6 and C7. The O···H6-C6 interaction was calculated to be slightly stronger than the O···H7-C7 interaction, with second order stabilisation energies of 0.63 and 0.54 kJ mol^{-1} respectively even though the ωB97X-D/aug-cc-pVQZ r_e geometry predicts an interatomic distance between O and the nearest H6 (2.882 Å) that is greater than that between O and the nearest H7 (2.729 Å). On fitting the r_0 parameters shown in Table 5, the derived separation between O and the nearest H6 is 2.926(3) Å and that between O and the nearest H7 is 2.765(3) Å. The natural bond orbitals imply that the orientation of the interaction between the O lone pair and H6-C6 is more favourable than that between the O lone pair and H7-C7. It was mentioned earlier that the hydrogen bond angle within this complex is found to be non-linear ($\angle$(O-H_b···N) = 163.3(52)°). The weak interactions described are apparently sufficiently strong to result in the observed non-linearity.

The NBO analysis of 2-ET···$(H_2O)_2$ (Table S40) reveals that the largest $E^{(2)}$ contribution corresponds to the interaction between the lone pair on N and antibonding σ*(H_{1b}-O1) orbital of the first water molecule. For the dihydrate complex this interaction was calculated to have a second order stabilisation energy of 64.39 kJ mol^{-1}, which is significantly higher than the energy of the same interaction within 2-ET···H_2O. The NCI analysis identified the presence of a second relatively strong hydrogen bond within the 2-ET···$(H_2O)_2$ complex, between the two water molecules. This interaction between a lone pair of O1 and the antibonding σ*(H_{2b}-O2) orbital is calculated to have a second order stabilisation energy of 51.04 kJ mol^{-1}. The magnitude of $E^{(2)}$ indicates that the N···H_{1b}-O1 hydrogen bond is stronger than the O1···H_{2b}-O2 interaction which is consistent with an earlier study of thiazole···$(H_2O)_2$.[11] The NBO analysis computed interaction energies of weaker hydrogen bonds between O atoms of the water molecules and hydrogen atoms on the ethyl group. The lone pair of O2 interacts principally with the antibonding orbital, σ*(C6-H6), with a much lesser contribution made by σ*(C7-H7). The second order stabilisation energy for the interaction of O2 with σ*(C6-H6) is 3.39 kJ mol^{-1}. On fitting the r_0 parameters shown in Table 6, the derived separation between O2 and the nearest H6 atom is 2.608(9) Å whereas O1 is 2.963(15) Å from the nearest H7 and 3.355(12) Å from the nearest H6. The relatively high strength of the N···H_{1b}-O1 hydrogen bond in 2-ET···$(H_2O)_2$ compared with that in 2-ET···H_2O, and also the fact that the weaker interactions (involving the ethyl group) are stronger within 2-ET···$(H_2O)_2$ than

within 2-ET···H_2O, confirms that cooperative hydrogen bonding effects are significant in the dihydrate.

Discussion

Analysis of the microwave spectra recorded for seven isotopologues of the 2-ET molecule has allowed the lowest-energy conformer to be identified as having C_1 symmetry. The dihedral angle, ∠(S-C2-C6-C7), is −98.6(10)° when determined from the experimentally-derived r_s coordinates and −110° when calculated at the ωB97X-D/aug-cc-pVQZ level. It is interesting to empirically review the factors that influence the value of this angle with reference to results obtained for comparator molecules. In the discussion that follows, "rotation of the ethyl group relative to the ring plane" should be understood to mean rotation about the axis of the C–C bond that connects the C_2H_5 group to a carbon atom within the aromatic ring of the molecule or complex under discussion.

The lowest-energy conformer of ethylbenzene was identified as being C_1 with the ethyl group rotated relative to the ring plane by 90°.[5] This is unsurprising given the high symmetry of benzene and that this configuration minimises steric hindrance by orienting the C_2H_5 group away from hydrogen atoms attached to the ring. Each of thiazole and furan is significantly less symmetrical than benzene. A recent experiment characterised a C_1 conformer of 2-ethylfuran through experiments performed using helium backing gas.[7] It was found that the ethyl group is rotated relative to the furan ring plane by 63.31(64)° (determined from r_s coordinates) in this molecule. The difference between ∠(O1-C2-C6-C7) = 63.31(64)° for 2-ethylfuran and ∠(S-C2-C6-C7) = −98.6(10)° for 2-ET implies that the identities of the heteroatoms significantly affect the molecular geometries of these molecules. The ethyl group is rotated toward O and away from C3 in the observed C_1 conformer of 2-ethylfuran. It is rotated slightly towards N and away from S in the lowest-energy conformation of 2-ET. In each of 2-ethylfuran and 2-ET, therefore, the direction of the ethyl group rotation apparently moves the CH_3 group closer to the more electronegative atom (oxygen in 2-ethylfuran and nitrogen in 2-ET). However, the symmetry of interactions between electronic orbitals on the ring and on the ethyl group will also have an effect. On basis of the empirical observations noted above, it is not possible to say whether (through-space) electrostatic effects or (through-bond) electronic effects are more significant.

Recent studies of conformations adopted by ethylaniline isomers[6] provide further insight. The dihedral angles that describe rotation of the ethyl group relative to the ring plane are 87.37(93)° and 91.3(17)° in 3-ethylaniline and 4-ethylaniline respectively. The ethyl group is remote from (and respectively meta or para to) the amine group in these molecules. The ∠(C8-C7-C2-C1) dihedral was calculated to be 75.59(82)° (from the r_s coordinates) for 2-ethylaniline where the ethyl group is ortho to the exocyclic amine group. It was suggested that a weak electrostatic interaction between the ethyl group and the nitrogen atom of the amine group leads to the deviation of ∠(C8-C7-C2-C1) from 90° for this molecule. The overall picture is that the geometries observed for C_1 conformers of ethylated aromatics broadly depend on the symmetries of the ethyl and aromatic groups in relation to each other. Deviation from the geometry of ethylbenzene, in which the ethyl group and the ring are mutually perpendicular (~90°), is observed for 2-ET, 2-ethylfuran and 2-ethylaniline. In each of these molecules, the ethyl group is bound to an asymmetric aromatic ring. On the other hand, the relevant dihedral angles in each of 3-ethylaniline and 4-ethylaniline are very close to that seen in ethylbenzene. This is consistent with these three molecules each being similar in respect of the symmetry of the ethyl group environment.

A good starting point for discussion of the geometry of the observed conformer of the 2-ET···H_2O is provided by recent work that studied imidazole-, thiazole-, methylthiazole- and methylimidazole-containing monohydrates. The water molecule binds to the pyridinic nitrogen and forms a weak hydrogen bond with either a hydrogen atom or CH_3 group on a neighbouring ring position in each of these complexes. As shown in Table 7, the various complexes can be divided into two groups according to the values of geometrical parameters. In each of imidazole···H_2O[1] and thiazole···H_2O[3] as well as *N*-methylimidazole···H_2O[2] and 5-methylthiazole···H_2O[4] (where the CH_3 group is remote from the binding position of the H_2O molecule) the geometrical parameters which describe the interaction between the heteroaromatic ring and H_2O are very similar. The length of the hydrogen bond,

Table 7. Comparison of experimentally-determined (r_0) structural parameters for complexes formed between 5-membered *N*-heterocyclic rings and H_2O.

Complex[a]	[H-bond donor on het. ring][b]	$r(H_b\cdots N)$/Å	∠(H_b···N-C2)/°	∠(O-H_b···N)/°
Imidazole···H_2O	C–H on C2	1.927(27)[c]	99.9(41)	172.1(26)
N-methylimidazole···H_2O	C–H on C2	1.922(4)	101.0(16)	177(5)
Thiazole···H_2O	C–H on C2	1.977(7)	95.6(4)	168.9(1)
5-methylthiazole···H_2O	C–H on C2	2.0037(42)	99.40(78)	166.0(23)
2-methylimidazole···H_2O	C–CH_3 on C2	1.923(5)	116.9(9)	166.3(28)
2-ET···H_2O	C–CH_2CH_3 on C2	1.983(13)	115.1(17)	163.3(52)
4-methylthiazole···H_2O	C–H_3 on C4	2.0296(68)	134.7(14)[d]	167.4(44)

[a] Results for imidazole···H_2O, *N*- and 2-methylimidazole···H_2O, 4- and 5-methylthiazole complexes from refs [1, 2 and 4] respectively. Results for thiazole···H_2O following re-analysis presented in ref [4] using data provided in ref [3]. [b] Indicates the atom or group of the heteroaromatic subunit which acts as the hydrogen bond donor in the secondary (weaker) hydrogen bond within the complex. [c] Uncertainties in parentheses are those quoted in the primary source.

$r(H_b\cdots N)$ ranges from 1.927(77) Å to 2.0037(42) Å and is observed to be slightly shorter for imidazole-containing complexes than for thiazole-containing complexes; the $\angle(H_b\cdots N\text{-}C2)$ angle ranges from 95.6(4)° to 101.0(16)°; and the $\angle(O\text{-}H_b\cdots N)$ angle ranges from 166.0(23)° to 177(5)° within this group. The $\angle(H_b\cdots N\text{-}C2)$ angle determined for 2-ET···H_2O during the present work is greater by ~15° than the range identified for the complexes within the first group.

The second group of monohydrates includes 2-methylimidazole···H_2O[2] and 4-methylthiazole···H_2O.[4] These complexes adopt somewhat different geometries (particularly in respect of the $\angle(H_b\cdots N\text{-}C2)$ angle) from those in the first group because they allow for H_2O to interact with a CH_3 group substituted onto either the 2- or 4-position of the ring. Interactions between H_2O and the ethyl group are expected within 2-ET···H_2O which contains the 2-ET monomer sub-unit in a C_1 conformation. The NBO analysis of the present work found that the oxygen lone pairs interact with each of σ*(C7-H7) and σ*(C6-H6) on the ethyl group and that each of these interactions makes a similar contribution to the overall stabilisation energy of the complex. The implication is that weak hydrogen bonds between the H_2O molecule and the hydrogens of the ethyl group cause the values of geometrical parameters for 2-ET···H_2O to be very similar to those found for 2-methylimidazole···H_2O as demonstrated by Table 7. This similarity occurs even while the positions and orientations of the C–H bonds within the C_2H_5 group of 2-ET···H_2O are somewhat different to those found within the CH_3 of 2-methylimidazole···H_2O. The $\angle(O\text{-}H_b\cdots N)$ angles of the complexes featured in Table 7 are generally somewhat less than 180° whereas a linear configuration (i.e. implying $\angle(O\text{-}H_b\cdots N) = 180°$) would be expected if only a single hydrogen bond formed between the two sub-units. The $\angle(H_b\cdots N\text{-}C2)$ angle in 4-methylthiazole···H_2O is somewhat greater than found for either 2-methylimidazole···H_2O or 2-ET···H_2O because the H_2O sub-unit is positioned to interact with the CH_3 group in the 4-position (rather than the 2-position) in the former.

The geometry of 2-ET···$(H_2O)_2$ has been shown to contain two strong and one weak hydrogen bonds. The water dimer sub-unit donates a hydrogen bond to the nitrogen while accepting a weak hydrogen bond from one or more C–H bonds. This is also true of the geometries of thiazole···$(H_2O)_2$ and phenanthridine···$(H_2O)_2$ which have been studied previously.[11,43] The r(O1···O2) distances in these three complexes are 2.894(21) Å, 2.826(33) Å and 2.85(1) Å respectively which compares with 2.976(10) Å for the isolated water dimer.[44] Evidently, cooperative effects shorten the r(O1···O2) distance relative to that found in the isolated water dimer in each of the above complexes. The broader trend for a series of related complexes was analysed within a recent work.[11] The water dimer is able to more effectively bridge the distance between the nitrogen and C–H bonds on the ethyl group than is the H_2O monomer. Consequently, the $\angle(O1\text{-}H_{1b}\cdots N)$ angle calculated for the r_e geometry of 2-ET···$(H_2O)_2$ is 174° which is greater than the same angle within the monohydrate complex (which is 163.3(52)°) and hence closer to the linear configuration that is optimal for a strong interaction. The ωB97X-D calculations (of r_e parameters) find that r(O1···N) is slightly shorter (by 0.07 Å) in 2-ET···$(H_2O)_2$ than in 2-ET···H_2O while the shortening implied by the r_0 results is 0.11 Å. The NBO analysis finds the second order stabilisation energy associated with this bond to be higher in 2-ET···$(H_2O)_2$ (64.4 kJ mol^{-1}) than in the monohydrate, 2-ET···H_2O (40.7 kJ mol^{-1}). The $\angle$(O1···N-C2) angle is determined to be 109.726(91)°, 120.55(15)°, 91.98(10)° and 106.5(49)° in the r_0 geometries of 2-ET···H_2O, 2-ET···$(H_2O)_2$, thiazole···H_2O and thiazole···$(H_2O)_2$ respectively. This series illustrates that the identity of the group at the 2-position of the thiazole ring has a clear and predictable effect on the position of the coordinating H_2O or $(H_2O)_2$ sub-unit; and that the effect of adding a second H_2O molecule to the molecular geometries of each of 2-ET···H_2O and thiazole···H_2O is similar. An interaction between the O atom of the first water molecule and C2-H2 was not identified in an NBO analysis of thiazole···$(H_2O)_2$, suggesting any computed interaction was too weak to be isolated at the sensitivity of the analysis (a threshold of 0.21 kJ mol^{-1} was used). On the other hand, the NCI and NBO analyses of 2-ET···$(H_2O)_2$ reveal some evidence of weak interactions between the O atom of the second water molecule and the two hydrogens on the ethyl group.

The ωB97X-D/aug-cc-pVQZ calculated results for the $\angle$(S-C2-C6-C7) dihedral angle vary significantly across the 2-ET monomer, 2-ET···H_2O and 2-ET···$(H_2O)_2$ series. Unfortunately, experimental values of this parameter are not available for 2-ET···H_2O and 2-ET···$(H_2O)_2$ because the spectra of isotopologues containing heavy atom isotopic substitutions within the 2-ET sub-unit were not available for these complexes. From the experiments and calculations performed herein, it is not possible to say whether the variation of this parameter is primarily a consequence of geometric distortions introduced by weak hydrogen bonds between the ethyl group and H_2O sub-units, or whether the effect of the strong hydrogen bond at the nitrogen is to induce changes in the electronic orbitals of the aromatic ring which also contribute to the identified change in this parameter.

Conclusions

Molecular geometries of 2-ET and two weakly-bound complexes formed by this molecule with water, 2-ET···H_2O and 2-ET···$(H_2O)_2$, have been characterised using microwave spectroscopy. Only one conformer of each of these species was identified during experiments which used argon or neon backing gases. The angle which defines the rotation of the ethyl group relative to the plane of the thiazole ring, $\angle$(S-C2-C6-C7), was determined to be −98.6(10)° from r_s coordinates of the isolated 2-ET molecule, consistent with a C_1 conformation. The molecule adopts a similar geometry (which is also C_1) when subsumed into the 2-ET···H_2O and 2-ET···$(H_2O)_2$ complexes, consistent with the results of quantum chemical calculations. Each of 2-ET···H_2O and 2-ET···$(H_2O)_2$ contains a strong hydrogen bond between an O–H of H_2O and the nitrogen atom; and one or more weaker hydrogen bonding interactions between the O of H_2O and C–H bonds of the ethyl group. The $\angle$(O···N-C2) angle is significantly greater for each of 2-ET···H_2O and 2-ET···$(H_2O)_2$ than for its thiazole-containing analogue. Cooperativity within the hydrogen bonding network results in a shorter and stronger primary hydrogen bond

for 2-ET···$(H_2O)_2$ than for 2-ET···H_2O and also a reduction in the *r*(O1···O2) distance compared with that in the isolated water dimer.

Acknowledgements

The authors acknowledge the Engineering and Physical Sciences Research Council for a DTA studentship awarded to C.N.C. and the European Research Council for project funding (Grant No. CPFTMW-307000).

Conflict of Interests

The authors declare no conflict of interest.

Data Availability Statement

The data that support the findings of this study are available from the corresponding author upon reasonable request.

Keywords: thiazole · rotational spectroscopy · microwave spectroscopy · hydrogen bonding · 2-ethylthiazole

[1] E. Gougoula, D. J. Cole, N. R. Walker, *J. Phys. Chem. A.* **2020**, *124*, 2649–2659.
[2] E. Gougoula, C. N. Cummings, C. Medcraft, J. Heitkämper, N. R. Walker, *Phys. Chem. Chem. Phys.* **2022**, *24*, 12354–12362.
[3] W. Li, J. Chen, Y. Xu, T. Lu, Q. Gou, G. Feng, *Spectrochim. Acta Part A* **2020**, *242*, 118720.
[4] C. N. Cummings, I. Kleiner, N. R. Walker, *J. Phys. Chem. A.* **2023**, *127*, 8133–8145.
[5] W. Caminati, D. Damiani, G. Corbelli, B. Velino, C. W. Bock, *Mol. Phys.* **1991**, *74*, 885–895.
[6] J. Wang, S. Herbers, P. Buschmann, K. Lengsfeld, J.-U. Grabow, G. Feng, Q. Gou, *Chin. J. Chem. Phys.* **2020**, *33*, 119–124.
[7] H. V. L. Nguyen, *J. Mol. Struct.* **2020**, *1208*, 127909.
[8] E. Gougoula, C. Medcraft, J. Heitkämper, N. R. Walker, *J. Chem. Phys.* **2019**, *151*, 144301.
[9] W. Jäger, H. Mäder, *Z. Naturforsch. A.* **1987**, *42*, 1405–1409.
[10] W. Jäger, H. Mäder, *J. Mol. Struct.* **1988**, *190*, 295–305.
[11] E. Gougoula, C. N. Cummings, Y. Xu, T. Lu, G. Feng, N. R. Walker, *J. Chem. Phys.* **2023**, *158*, 114307.
[12] D. Loru, M. A. Bermúdez, M. E. Sanz, *J. Chem. Phys.* **2016**, *145*, 074311.
[13] D. P. Zaleski, S. L. Stephens, N. R. Walker, *Phys. Chem. Chem. Phys.* **2014**, *16*, 25221–25228.
[14] G. A. Cooper, C. Medcraft, J. D. Littlefair, T. J. Penfold, N. R. Walker, *J. Chem. Phys.* **2017**, *147*, 214303.
[15] D. M. Bittner, S. L. Stephens, D. P. Zaleski, D. P. Tew, N. R. Walker, A. C. Legon, *Phys. Chem. Chem. Phys.* **2016**, *18*, 13638–13645.
[16] Gaussian 09 (Revision D.01) M. J. Frisch, G. W. Trucks, H. B. Schlegel, G. E. Scuseria, M. A. Robb, J. R. Cheeseman, G. Scalmani, V. Barone, B. Mennucci, G. A. Petersson, H. Nakatsuji, M. Caricato, X. Li, H. P. Hratchian, A. F. Izmaylov, J. Bloino, G. Zheng, J. L. Sonnenberg, M. Hada, M. Ehara, K. Toyota, R. Fukuda, J. Hasegawa, M. Ishida, T. Nakajima, Y. Honda, O. Kitao, H. Nakai, T. Vreven, J. Montgomery, J. A., J. E. Peralta, F. Ogliaro, M. Bearpark, J. J. Heyd, E. Brothers, K. N. Kudin, V. N. Staroverov, T. Keith, R. Kobayashi, J. Normand, K. Raghavachari, A. Rendell, J. C. Burant, S. S. Iyengar, J. Tomasi, M. Cossi, N. Rega, J. M. Millam, M. Klene, J. E. Knox, J. B. Cross, V. Bakken, C. Adamo, J. Jaramillo, R. Gomperts, R. E. Stratmann, O. Yazyev, A. J. Austin, R. Cammi, C. Pomelli, J. W. Ochterski, R. L. Martin, K. Morokuma, V. G. Zakrzewski, G. A. Voth, P. Salvador, J. J. Dannenberg, S. Dapprich, A. D. Daniels, O. Farkas, J. B. Foresman, J. V. Ortiz, J. Cioslowski, D. J. Fox, *Gaussian, Inc., Wallingford*, CT, **2013**.
[17] B. Miehlich, A. Savin, H. Stoll, H. Preuss, *Chem. Phys. Lett.* **1989**, *157*, 200–206.
[18] S. H. Vosko, L. Wilk, M. Nusair, *Can. J. Phys.* **1980**, *58*, 1200–1211.
[19] A. D. Becke, *J. Chem. Phys.* **1993**, *98*, 5648–5652.
[20] S. Grimme, M. Steinmetz, *Phys. Chem. Chem. Phys.* **2013**, *15*, 16031–16042.
[21] S. Grimme, S. Ehrlich, L. Goerigk, *J. Comput. Chem.* **2011**, *32*, 1456–1465.
[22] A. D. Becke, E. R. Johnson, *J. Chem. Phys.* **2005**, *123*, 154101.
[23] R. A. Kendall, T. H. Dunning, R. J. Harrison, *J. Chem. Phys.* **1992**, *96*, 6796–6806.
[24] T. H. Dunning, *J. Chem. Phys.* **1989**, *90*, 1007–1023.
[25] F. Weigend, R. Ahlrichs, *Phys. Chem. Chem. Phys.* **2005**, *7*, 3297–3305.
[26] F. Weigend, *Phys. Chem. Chem. Phys.* **2006**, *8*, 1057–1065.
[27] C. Møller, M. S. Plesset, *Phys. Rev.* **1934**, *46*, 618–622.
[28] J.-D. Chai, M. Head-Gordon, *Phys. Chem. Chem. Phys.* **2008**, *10*, 6615–6620.
[29] R. S. Ruoff, T. D. Klots, T. Emilsson, H. S. Gutowsky, *J. Chem. Phys.* **1990**, *93*, 3142–3150.
[30] S. R. Domingos, C. Pérez, C. Medcraft, P. Pinacho, M. Schnell, *Phys. Chem. Chem. Phys.* **2016**, *18*, 16682–16689.
[31] J. K. G. Watson, *J. Chem. Phys.* **1968**, *48*, 4517–4524.
[32] C. M. Western, *J. Quant. Spectrosc. Radiat. Transfer.* **2017**, *186*, 221–242.
[33] L. Nygaard, E. Asmussen, J. H. Høg, R. C. Maheshwari, C. H. Nielsen, I. B. Petersen, J. Rastrup-Andersen, G. O. Sørensen, *J. Mol. Struct.* **1971**, *8*, 225–233.
[34] B. Bak, D. Christensen, L. Hansen-Nygaard, J. Rastrup-Andersen, *J. Mol. Spectrosc.* **1962**, *9*, 222–224.
[35] J. U. Grabow, H. Hartwig, N. Heineking, W. Jäger, H. Mäder, H. W. Nicolaisen, W. Stahl, *J. Mol. Struct.* **2002**, *612*, 349–356.
[36] T. Nguyen, V. Van, C. Gutlé, W. Stahl, M. Schwell, I. Kleiner, H. V. L. Nguyen, *J. Chem. Phys.* **2020**, *152*, 134306.
[37] Z. Kisiel, "*PROSPE – Programs for ROtational SPEctroscopy*" can be found under http://info.ifpan.edu.pl/~kisiel/prospe.htm, **1999** (accessed 14 December 2023).
[38] C. C. Costain, *Trans. Am. Crystallogr. Assoc.* **1966**, *2*, 157–164.
[39] Z. Kisiel, *J. Mol. Spectrosc.* **2003**, *218*, 58–67.
[40] E. R. Johnson, S. Keinan, P. Mori-Sánchez, J. Contreras-García, A. J. Cohen, W. Yang, *J. Am. Chem. Soc.* **2010**, *132*, 6498–6506.
[41] A. E. Reed, L. A. Curtiss, F. Weinhold, *Chem. Rev.* **1988**, *88*, 899–926.
[42] T. Lu, F. Chen, *J. Comput. Chem.* **2012**, *33*, 580–592.
[43] D. Loru, A. L. Steber, P. Pinacho, S. Gruet, B. Temelso, A. M. Rijs, C. Pérez, M. Schnell, *Phys. Chem. Chem. Phys.* **2021**, *23*, 9721–9732.
[44] J. A. Odutola, T. R. Dyke, *J. Chem. Phys.* **1980**, *72*, 5062–5070.

Manuscript received: January 3, 2024
Revised manuscript received: February 2, 2024
Accepted manuscript online: February 5, 2024
Version of record online: ■■, ■■

RESEARCH ARTICLE

Microwave (2–18 GHz) spectra of the isolated 2-ethylthiazole molecule, and isolated complexes of 2-ethylthiazole···H_2O and 2-ethylthiazole···$(H_2O)_2$ are analysed. The geometry of each hydrate complex contains a non-linear, N···H–O, hydrogen bond between an O–H of H_2O and the nitrogen atom while the O atom of the water molecule(s) interacts weakly with the ethyl group.

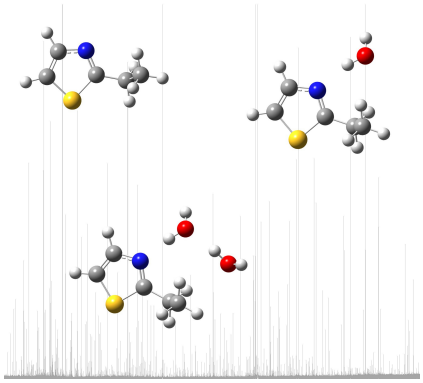

*C. N. Cummings, N. R. Walker**